Time-Delay-Integration Architectures in CMOS Image Sensors

Gérald Lepage, Jan Bogaerts, and Guy Meynants

***Abstract*—Difficulty and challenges of implementing time-delay-integration (TDI) functionality in a CMOS technology are studied: synchronization of the samples forming a TDI pixel, adder matrix outside the array, and addition noise. Existing and new TDI sensor architecture concepts with snapshot shutter, rolling shutter, or orthogonal readout are presented. An optimization method is then introduced to inject modulation transfer function and quantum efficiency specification in the architecture definition. Moderate spatial and temporal oversamplings are combined to achieve near charge-coupled device (CCD) class performances, resulting in an acceptable design complexity. Finally, CCD and CMOS dynamic range and signal-to-noise ratio are conceptually compared.**

***Index Terms*—Dynamic modulation transfer function (MTF), image sensor, optical transfer functions, pushbroom, time-delay integration (TDI).**

I. Introduction

TIME-DELAY integration (TDI) is a particular imaging mode used for decades and typically implemented with 2-D charge-coupled devices (CCDs) [1], [2]. When the scene is moving with respect to the detector, the resulting image will be blurred. In many imaging applications, the image scene moves relative to the detector with a constant or predictable velocity, for instance, in machine vision applications, document scanning, and roll or conveyer belt inspection systems. Another well-known application is pushbroom imaging for Earth observation from satellite or aircraft. In such cases, a 1-D array can be used to generate 2-D images by repeatedly exposing and integrating on the single row of pixels while moving the detector in a direction that is orthogonal to the long dimension of the array. The direction of the motion is called "along-track," while the direction that is orthogonal to this motion direction is called "across-track." One significant problem of the scanned reading mode is that because of the relative motion that the exposure time for each image "slice" is limited, restricting the image performance in terms of signal-to-noise ratio (SNR).

In line scan applications where the light level is low or where the relative speed of the movement is large, TDI image sensors are useful. In a TDI sensor, a 2-D pixel array is used. The pixel signals delivered by the pixels of the same column (along-track direction) are, in that case, adequately delayed and added synchronously with the optical scanning. Thus, the light from a given point in the scene impinges successively on each pixel of the given corresponding column. As the light of the scene impinges on each row in succession, the signals from each of the rows are added to increase the final SNR. A simple example of the TDI principle is shown in Fig. 1.

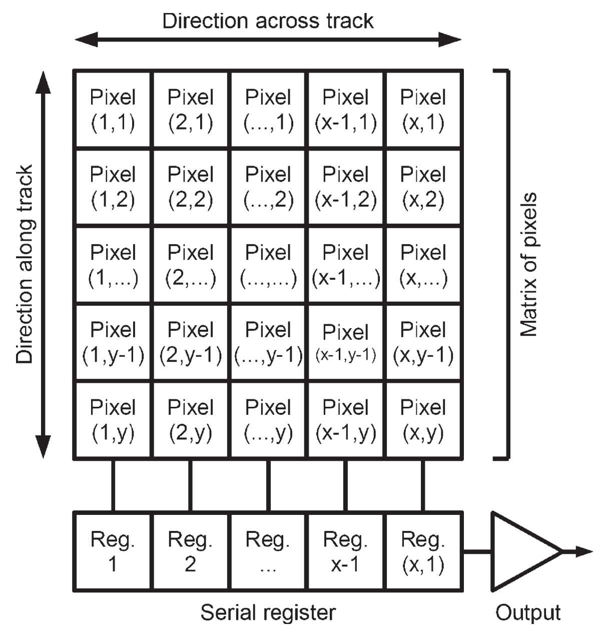

Fig. 1. Schematic illustration of the TDI mode of operation with a CCD device.

The TDI principle has typically been addressed with CCD sensors where the TDI functionality is more or less intrinsically available by shifting the charge packets along the CCD synchronously with the moving image. This addition process is noise free in a CCD. This is not so easily implemented in CMOS APS. In particular, it is not possible to follow the image movement on the sensor by synchronously shifting charges during the integration, potentially resulting in a modulation transfer function (MTF) degradation. In addition, as the signal is converted to voltage directly inside the pixel, adders are typically required outside the pixel matrix. However, there are compelling reasons to implement this functionality in CMOS because of the potential advantages of process accessibility, reduced cost, additional circuit functionality on-chip, robustness to ionizing radiation, simpler system design, etc. This paper discusses the implementation of TDI functionality in CMOS active pixel image sensors. Section II looks into various architectural variants of CMOS image sensors with TDI functionality. Section III discusses how the optical performance of CMOS TDI sensors can be optimized for optimal dynamic

Manuscript received January 6, 2009; revised July 8, 2009. First published September 29, 2009; current version published October 21, 2009. The review of this paper was arranged by Editor P. Magnan.
The authors are with CMOSIS, 2600 Antwerpen, Belgium (e-mail: gerald.lepage@cmosis.com).
Digital Object Identifier 10.1109/TED.2009.2030648

MTF and sensitivity, and how read noise and dynamic range relate to the number of TDI stages in CMOS TDI sensors.

II. Architecture of CMOS TDI Sensors

A. Architectural Requirements for TDI Functionality

TDI functionality requires low-noise addition of pixels in the along-track direction. This sets forward several requirements which must be fulfilled concurrently:

1) low-noise pixel readout;
2) on-chip addition circuitry, either in the digital or analog domain;
3) synchronous signal capture of the image for all pixels in the along-track direction.

As mentioned before, CCDs fulfill each of these requirements by construction. Addition is done noise-free in the charge domain, and all pixels acquire data synchronously. CMOS active pixel image sensors can be read out with low noise by correlated double sampling in four-transistor pinned photodiodes. However, such pixels have a rolling shutter, requiring temporal over- or undersampling as explained hereinafter. Operating modes with snapshot shutter exist in several CMOS shutter architectures, but these are without correlated double-sampling readout. The combination of these features, as required for TDI operation, is not straightforward. Another important feature of CCD is the selection of the number of vertical stages to adjust the sensor sensitivity to the scene content. This is easily controlled in CMOS by changing the timing and reading out only the samples needed.

B. Synchronous Shutter Pixels

An object is successively acquired by each pixel of column. Samples are read out and summed together to form the final pixel, owing to an array of adders (Fig. 2). Each pixel must have acquired exactly the same object; otherwise, the image sharpness will be degraded. If the pixel integration time matches the travel time of the scene from one pixel to the next one, then all pixels must be operated synchronously. This cannot be done with rolling-shutter active CMOS pixels as they share the same column bus and only one row can be read at the time. If pixels are regularly distributed in the matrix, a straightforward solution consists in using pipeline snapshot shutter pixels [3]. All pixels start and stop integrating simultaneously. Samples are stored in an in-pixel memory, typically a capacitor, and a new integration period starts while the matrix is read out row by row.

The timing principle is shown in Fig. 3 with 5 pixels. As the same scene element is successively acquired by pixels 1–5, the intermediate result is stored in an adder. When the fifth sample has been added, the corresponding adder is read out from the sensor and reused for a new pixel.

Many snapshot shutter pixel architectures have been reported. They are more complex than classical rolling-shutter pixels because of the extra memory element inside the pixel. This is limiting the quantum efficiency and the minimum feasible pixel pitch. Some global shutter pixel structures exhibit a relatively poor snapshot shutter efficiency which could af-

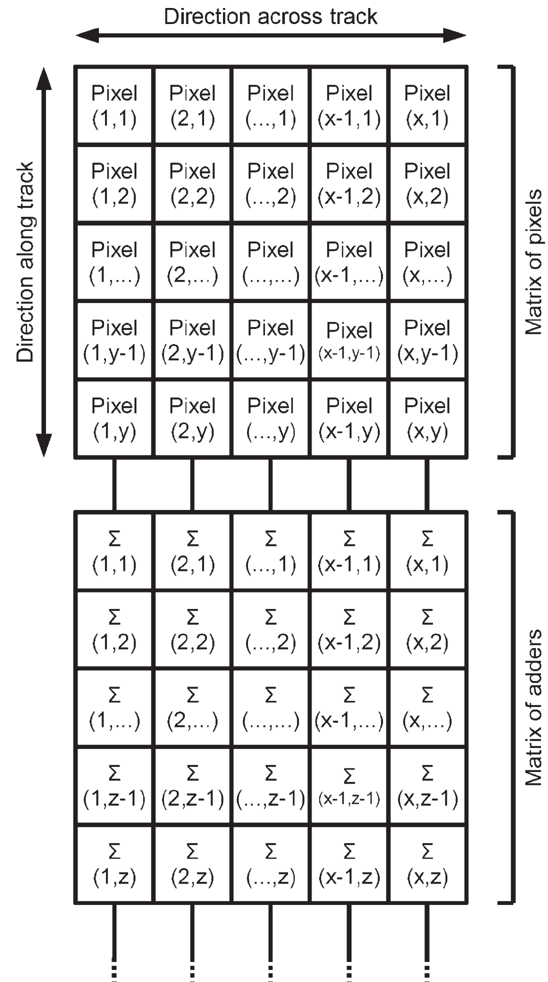

Fig. 2. Implementation of the TDI mode of operation with a CMOS device.

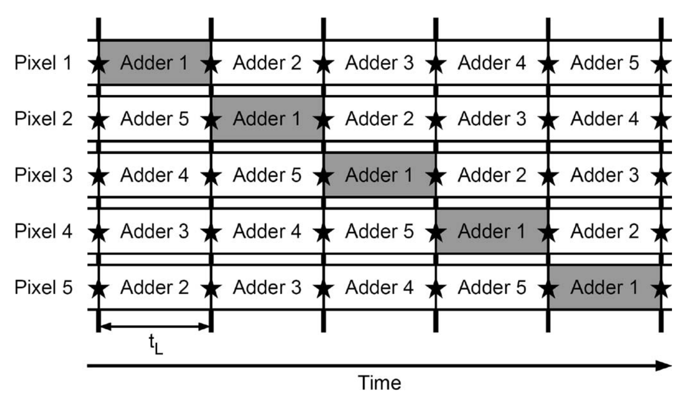

Fig. 3. Timing with snapshot shutter.

fect the overall image quality. Compact snapshot shutter pixel circuits do not cancel the kTC or reset noise of the floating diffusion node which converts the photocharge into a voltage signal. This high noise level degrades the dynamic range of the TDI signal.

C. Rolling-Shutter Readout

If the scene is temporally under- or oversampled, e.g., if the pixel integration time is different from the line time, then snapshot pixels are no more required. Samples added together

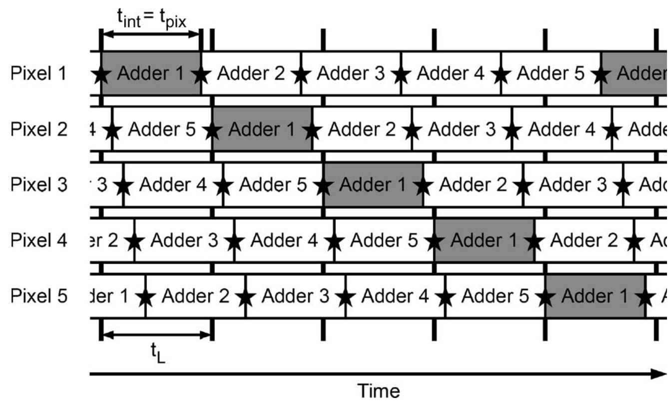

Fig. 4. Timing with rolling shutter.

to form the final pixel are still delayed by one line time t_L; however, two consecutive pixels are delayed by $t_{\mathrm{pix}} \neq t_L$ [4]. As a consequence, each pixel of a column is ending an integration period at a different time than any other; thus, it is possible to operate the matrix in rolling shutter as shown in Fig. 4 (stars are showing when a pixel needs to be read out). A three-transistor active pixel or a four-transistor active pixel with pinned diode is sufficient. These rolling-shutter pixels can be read out at lower noise levels with CDS, which is the main motivation to utilize them in CMOS TDI sensors.

D. Orthogonal Readout

In this paragraph, we discuss an alternative method to circumvent the problem of synchronization between pixels along track, on one hand, and to avoid the use of snapshot shutter pixels, on the other hand. In case the number of TDI stages is large or the line time is short, the multiplexing of the signals on the column bus as described in the previous paragraph can become complex. For the along-track rolling line shutter, the effective pixel pitch after TDI is correlated to the timing and must be carefully controlled to avoid display artifacts. Therefore, a rolling-shutter approach in the across-track direction is considered here. The timing of pixels within a column is then again simplified to the timing shown in Fig. 3.

Fig. 5 shows a sensor that can be used in a rolling-shutter mode while preserving synchronicity of integration times between pixels in the along-track direction. In the simplest form, the imager has readout buses in the across-track direction, and the readout circuitry is arranged to use the set of readout buses to read from a single column (along-track direction) of pixels during each reading operation. The readout circuitry can comprise analog or digital adders, or the pixel signal summation can be performed off-chip. The total pixel array still needs to be read out in a period shorter than or equal to the line time. With a rolling shutter in the across-track direction, the integration period start time of each column is offset from an integration period start time of any other column of the array, i.e., each column has a different integration period start time and a different integration period stop time from any other column of the array. However, all pixels of a column are integrating synchronously. This sequence will therefore result in an image with a nonorthogonal coordinate system, and the image has thus the form of a parallelogram, as shown in Fig. 6.

Two different modifications can be made to this architecture to alleviate its possible drawbacks. Typically, TDI imagers have a very elongated shape (large aspect ratio) with a limited number of pixels in the along-track direction. As a result, the multiplexing readout buses in the pixel array are long and heavily loaded, which will slow down multiplexing speed and increase power consumption. Each readout also requires some overhead time to sample the multiplexed signals into the readout circuits. Since the number of lines to be read out is large, the frame rate is also reduced. However, the integration period and frame readout time in TDI operation typically need to be relatively short. The large number of pixels attached to the readout buses can thus become problematic in the configuration as shown in Fig. 5.

In a more sophisticated architecture, the readout buses are provided in a layout which permits multiple columns of pixels to be read in parallel during each reading operation. One way of achieving this is to provide a larger set of readout buses, with each readout bus connecting a group of pixels which are positioned diagonally across the array. This is shown in Fig. 7. The sensor is also operated in a rolling-shutter mode, but multiple pointers are active in the across-track direction. This can drastically speed up the frame readout since the diagonal bus lines are short and multiple columns are read out simultaneously.

Second, a physical offset, in the along-track direction, is provided between pixels of the columns of the array with respect to pixels of other columns in the array. This is schematically shown in Fig. 8. The physical offset can be used to fully, or partially, compensate for the difference in integration period start times of the columns. The offset between each pair of columns is constant. Each row of pixels now has an axis which is nonorthogonal with respect to the axis of a column of pixels. The total accumulated shift of the columns over the complete detector (or part readout by single readout pointer) should correspond to the shift in integration time between first and last columns and the relative velocity of the scene. The shift in integration times between the columns is then fully compensated by the shift in physical layout of the columns. Finally, this would again result in an orthogonal sampling of the scene.

E. Addition in Digital Domain

The addition process in all of the previous architectures can be performed using analog accumulators [3] or eventually be made off-chip. Another possibility is to perform A-to-D conversion early in the signal chain and perform the addition in the digital domain. In case the required speed and accuracy can be reached in the ADC, this addition process turns out to be much simpler than that in the analog domain. In Fig. 9, we propose the use of a ramp ADC with a local counter. This counter is used in combination with a memory array. This architecture is inherently well suited for accumulation of multiple signals.

Prior to each pixel signal accumulation, the counter is initialized with the then already accumulated signal (the data from

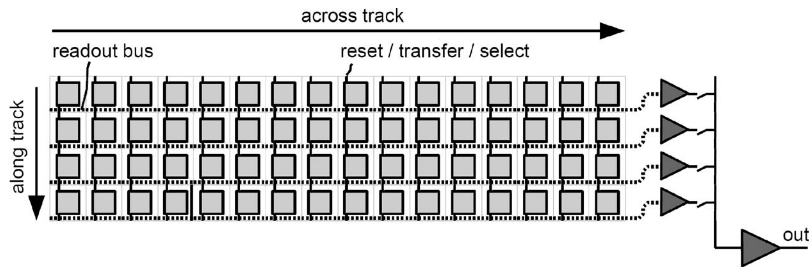

Fig. 5. Sensor architecture with rolling shutter in the across-track direction.

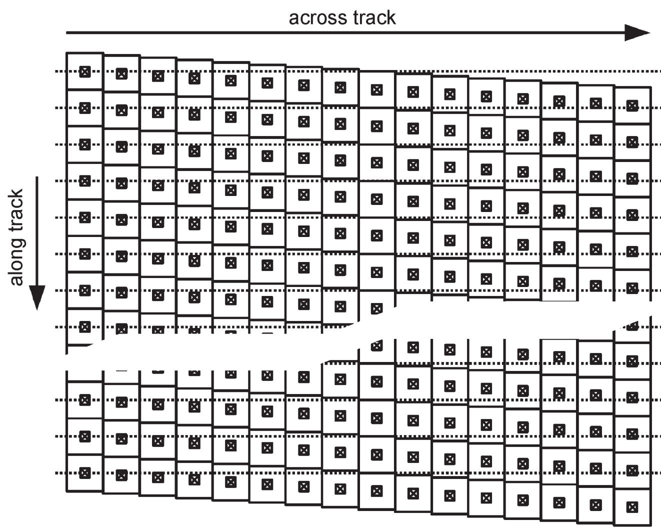

Fig. 6. Final image with a nonorthogonal coordinate system.

one memory location are read and written into the counter). The counter is then incremented according to the pixel value, and its output is again stored in the memory. Initializing the counter in the ADC to the previously accumulated value allows accumulation without the need for a separate adder, which can provide a considerable saving in area and complexity. Either the memory location of a TDI pixel (i.e., accumulated signal) is fixed (the data of the counter are written into the same memory location) or the location of the TDI pixel shifts through the memory array. In the first case, the memory is read out in a rolling readout sequence (readout pointer required). In the latter case, always the last memory location (holding the fully accumulated TDI signal) has to be read out.

Accumulation in the digital domain offers also some additional advantages. In CCD technology, the dynamic range is determined by the full well capacity of the pixel (or the output register in case its charge handling capacity would be lower) and the readout noise. Bright objects in the scene that saturate the pixel after accumulation in the pixel array but before readout (e.g., n_{TDI} lines in total, but pixel signal saturates after less than n_{TDI} additions) will not generate useful information. Since the TDI accumulation process does not necessarily happen within the pixel in the case of CMOS APS, the final charge handling capacity can be much larger than the full well charge of a single pixel. This also means that the charge handling capacity of a CMOS APS pixel in a TDI sensor can be made relatively small, which is, in general, beneficial for its noise performance (operation with high conversion gain with low read noise). The charge handling capacity will, in this case, be limited by the charge handling capacity of the accumulators. In the case of digital addition, the addition process can be controlled dynamically without much complexity. The idea is to check after each addition whether the next addition should take place or not. This can, for example, be implemented in the column at the counter level. The principle is shown in Fig. 10. If the counter value exceeds a certain (predefined or programmable) value, the addition of next pixel signals is suppressed, and the TDI depth (number of accumulations at which the threshold has been exceeded) is memorized (with no further memory access for following additions). This means that each pixel can have its own optimal TDI level and, at the same time, use the full dynamic range offered by the accumulator.

III. Optimizing Optical Performances

Several figures of merit (FOMs) can be defined for a TDI sensor. As the main goal of a TDI sensor is to increase the SNR, quantum efficiency $QE(\lambda)$ is important. Because the scene is not still during the acquisition, net or dynamic MTF MTF_{dyn} is also a key FOM. We will see that other parameters are linked to $QE(\lambda)$ and MTF_{dyn} when optimizing a TDI sensor in CMOS.

MTF_{dyn} is the product of the intrinsic MTF of the sensor MTF_{aperture}, defined by its aperture, and a motion-related factor MTF_{discrete} [1]. Other effects (charge diffusion, etc.) typically affect the MTF, but they are not taken in account there to simplify the analysis. In a CCD device, charges are moved *during* the integration in the direction along track by pixel subpitch steps, in an attempt to approximately follow the scene motion onto the device. Depending on the architecture, it is possible to get MTF_{discrete} very close to one at the pixel Nyquist frequency. For instance, a CCD with a four-phase nonoverlapping clock has four moves per line time (and per pixel pitch) and achieves an MTF_{discrete} of 0.974

$$MTF_{\mathrm{discrete}} = \mathrm{sinc}\left(\frac{\pi}{2 \cdot 4}\right) \approx 0.974. \tag{1}$$

Such charge transfer is not possible with a standard CMOS device. A straightforward implementation with a single addition step of adjacent pixels per line time exhibits an MTF_{discrete} of 0.64 at best

$$MTF_{\mathrm{discrete}} = \mathrm{sinc}\left(\frac{\pi}{2}\right) \approx 0.64. \tag{2}$$

The overall MTF could however be improved by reducing the aperture with a light shield like in [5] while keeping the

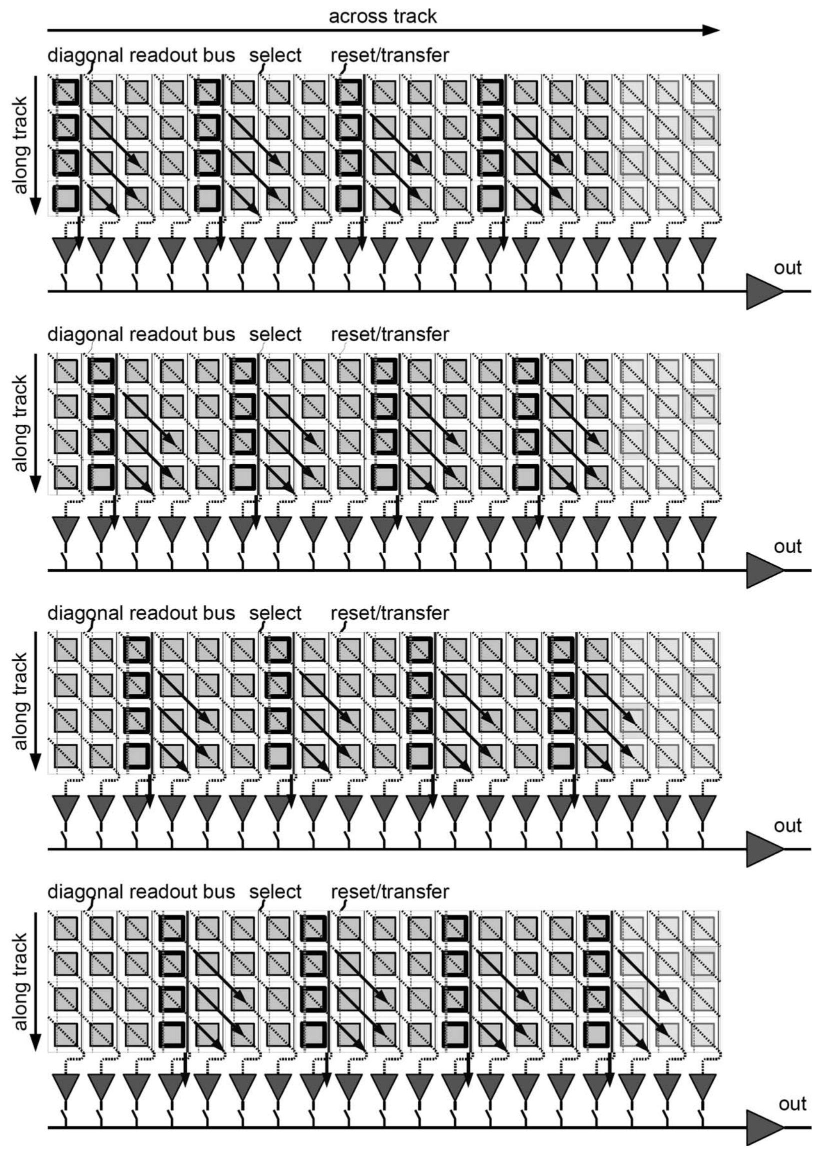

Fig. 7. Sensor architecture with rolling shutter in the across-track direction with diagonal readout bus lines. The figure shows the rolling sequence (left to right in the pixel array) with multiple active readout pointers. The pixels in bold integrate and are read out simultaneously.

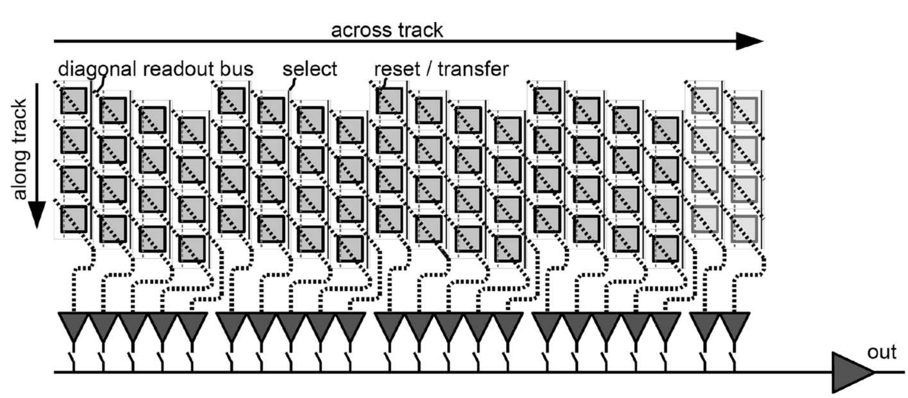

Fig. 8. Sensor architecture with rolling shutter in the across-track direction with diagonal readout bus lines. The neighboring columns show a physical offset in layout to compensate for the shift in integration periods.

pixel pitch unchanged. This results in a severe loss of quantum efficiency and thus SNR. Alternatively, the pixel pitch could be halved in the along-track direction, and the number of pixels doubled. This is roughly equivalent to a two-phase CCD and gives a discrete of 0.9. We are presenting a more elaborated optimization method in the next paragraph.

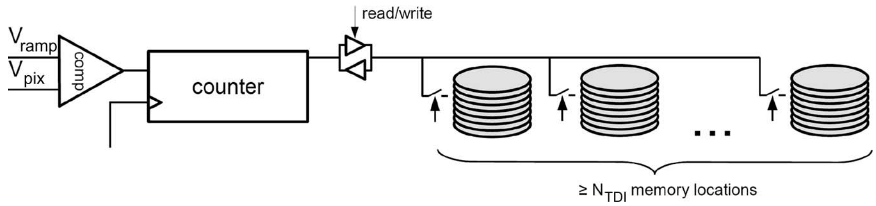

Fig. 9. Ramp ADC with a local counter.

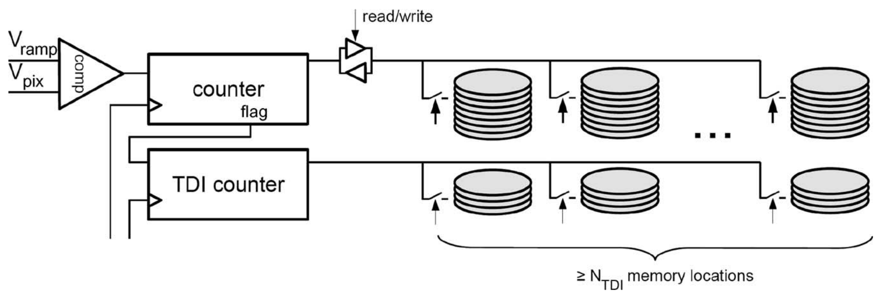

Fig. 10. Architecture with dynamically controlled n_{TDI}.

A. Quantum Efficiency and Dynamic MTF

In order to achieve the best quantum efficiency for a given pitch, a rolling-shutter active pixel is selected (typically three-transistor or four-transistor APS). Three conditions are required to enable proper TDI operation in this case:

1) synchronization of time-delayed samples of the same image acquired once by each pixel of a column;
2) timing requiring at any time readout of only one pixel per column, as only one pixel per column could be accessed at a time;
3) enabling temporal under- or oversampling of the image with respect to a reference sampling period defined as the pixel pitch divided by the image velocity on the sensor (not necessary with orthogonal readout).

In addition, it is desirable to tweak the operating point in order to achieve optimum performances with moderate extra design complexity. Pixel dimensions are shown in Fig. 11. The overall MTF MTF_{dyn} is the product of MTF_{aperture} and MTF_{discrete}, which can be calculated as in the following equations (see Table I for term explanation):

$$MTF_{\mathrm{aperture}} = \mathrm{sinc}\left(\frac{\pi}{2}\cdot\frac{p'_{\mathrm{acq}}}{p_{\mathrm{ref}}}\right) \tag{3}$$

$$MTF_{\mathrm{discrete}} = \mathrm{sinc}\left(\frac{\pi}{2}\cdot\frac{t_{\mathrm{int}}}{t_{L,\mathrm{ref}}}\right). \tag{4}$$

A solution with temporal oversampling has been reported (see [4] and [6]); however, in this implementation, the temporal oversampling ratio and the number of adders are linked to the number of TDI stages n_{TDI} as follows:

$$t_{\mathrm{pix}} = \frac{n_{\mathrm{TDI}}}{n_{\mathrm{TDI}}+1}\cdot t_L \tag{5}$$

$$n_{\mathrm{adders}} = n_{\mathrm{TDI}} + 1. \tag{6}$$

As a consequence, MTF_{dyn} is limited by construction to approximately 0.41 for large n_{TDI}, although this relationship between n_{TDI} and the temporal oversampling ratio is not mandatory:

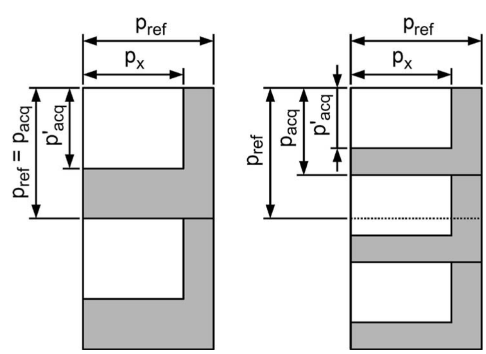

Fig. 11. Pitch definition (left) without and (right) with spatial oversampling in the along-track direction. Direction along track is vertical. Gray zones are not light sensitive.

$$\begin{aligned} MTF_{\mathrm{dyn}} &= MTF_{\mathrm{aperture}}\cdot MTF_{\mathrm{discrete}} \\ &= \mathrm{sinc}\left(\frac{\pi}{2}\right)\cdot\mathrm{sinc}\left(\frac{\pi}{2}\cdot\frac{n_{\mathrm{TDI}}}{n_{\mathrm{TDI}}+1}\right) \\ &\approx 0.41. \end{aligned} \tag{7}$$

Intuitively, it is easier to achieve a given MTF_{dyn} when MTF_{aperture} and MTF_{discrete} are equal. Interestingly enough, MTF_{aperture} does not depend on the shield width $(p_{\mathrm{ref}} - p_{\mathrm{acq}})$, so the overall MTF can be improved without degrading too much the quantum efficiency.

Suppose that we target an MTF_{dyn} of 0.6. Let's choose $MTF_{\mathrm{aperture}} = MTF_{\mathrm{discrete}}$ (it is not necessarily optimum in all cases). We then have:

$$p'_{\mathrm{acq}} = 0.77\cdot p_{\mathrm{ref}} \tag{8}$$

$$t_{\mathrm{int}} = t_{\mathrm{pix}} = 0.77\cdot t_{L,\mathrm{ref}}. \tag{9}$$

This results in both temporal and spatial oversamplings of 30% to achieve a CCD class MTF performance. At this point,

TABLE I
NOTATIONS

Symbol	Description
v	Scene displacement velocity on the sensor.
$QE(\lambda)$	Quantum efficiency.
Pix_{el}	Elementary pixel sample.
Pix_{TDI}	TDI pixel sample read out from the sensor, e.g. after summation.
p_x	Pixel pitch across track.
p_{ref}	Pixel pitch along track.
p_{acq}	Acquisition pitch (physical pitch at sensor level) along track.
p'_{acq}	Pixel opening along track.
t_L	Sampling period. It is the time between the acquisition of two consecutive samples of the scene by two adjacent physical pixels.
$t_{L,ref}$	Reference sampling period.
$t_{L,acq}$	Acquisition sampling period.
t_{int}	Pixel integration time.
t_{pix}	Pixel period.
t_{hold}	The data is available during t_{hold} on an adder after the last addition.
$n_{TDI,acq}$	Number of Pix_{el} added per Pix_{TDI}.
$n_{TDI,acq,max}$	Maximum number of Pix_{el} added per Pix_{TDI} for a given timing.
n_{adders}	Minimum number of adders required per column.
t_{stab}	Duration between the beginning and the end of respectively the first and the last elementary pixel samples of a TDI pixel sample.
$f_{ro,pix}$	Average row data rate.
$f_{ro,sensor}$	Average data rate after addition.
$\phi(\lambda)$	Given an incoming monochromatic light power per area $E(\lambda)$, an equivalent photocurrent could be calculated assuming 100 % quantum efficiency: $\phi(\lambda) = E(\lambda) \cdot \frac{\lambda \cdot q}{h \cdot c}$
$i_{ph,max}$	Maximum photocurrent possible per physical pixel, assuming $p'_{acq} = p_{acq}$.
Q_{TDI}	Charge accumulated in Pix_{TDI}.
f_N	Nyquist frequency $f_N = \frac{1}{2 \cdot p_{ref}}$.
$MTF_{aperture}$	Aperture MTF at f_N.
$MTF_{discrete}$	Discrete (velocity) MTF at f_N.
MTF_{dyn}	Dynamic (overall) MTF at f_N: $MTF_{dyn} = MTF_{aperture} \cdot MTF_{discrete}$

minimizing p_{acq} is minimizing the total acquisition time to achieve a given SNR or effectively increasing the quantum efficiency. Choosing p_{acq} that is slightly larger than p'_{acq} (extra space is needed for pixel routing) but smaller than p_{ref} is a good tradeoff:

$$p_{\text{acq}} = 0.89 \cdot p_{\text{ref}}. \tag{10}$$

It shall be noted that the image will need to be resampled to the target resolution because the effective pixel pitch after TDI is a function of spatial and temporal oversamplings.

The timing is now entirely defined. For a given illumination, an SNR FOM is $Q_{\text{TDI}} \cdot f_{\text{ro,sensor}}$, i.e., the amount of charges acquired per unit of time. This optimized sensor and a reference sensor with 100% fill factor and no oversampling are compared for the same $Q_{\text{TDI}} \cdot f_{\text{ro,sensor}}$ in Table II. As a consequence of the oversampling, more additions and adders are required for the optimized sensor. The stability or pointing time is slightly longer, i.e., the sensor size in the along-scan direction is slightly longer because the fill factor is less than 100%. This is not due to the oversampling technique but to the necessary blind areas in between pixels for routing with front-side illuminated CMOS sensors. The dynamic MTF is much better.

TABLE II
REFERENCE AND OPTIMIZED SENSOR COMPARISON

Parameter	Optimized	Reference
$n_{TDI,acq}$	13	10
t_{stab}	$11.3 \cdot t_{L,ref}$	$10 \cdot t_{L,ref}$
n_{adders}	14	10
MTF_{dyn}	0.6	0.41

B. Timing Example

We illustrate with figures a simple timing example with the following parameters:

$$n_{\text{TDI}} = 3 \tag{11}$$

$$p_{\text{acq}} = \frac{8}{13} \cdot p'_{\text{acq}} \tag{12}$$

$$t_{\text{int}} = \frac{2}{5} \cdot t_{L,\text{acq}} \tag{13}$$

$$t_{\text{pix}} = \frac{3}{5} \cdot t_{L,\text{acq}}. \tag{14}$$

Fig. 12 shows the scene projected onto the device at several time instants (the scene has a constant velocity from top to bottom). When an object is in a nonsensitive area, in between two pixel apertures, then the signal is lost (object drawn in gray). The signal is also lost when the pixel is not integrating, during reset for instance, as shown in Fig. 13. This duration can actually be reduced to a very small fraction of t_{pix}. In both figures, the successive acquisitions of a TDI sample by the 3 pixels of a column are delayed by $t_{L,\text{acq}}$ and perfectly matching. They are combined to a 3-D plot in Fig. 14. In this example, MTF_{discrete} equals 0.94.

C. Read Noise and Dynamic Range

Several sources contribute to the total read noise of a TDI CCD device. As the photocharge is converted into a voltage signal inside each pixel, all uncorrelated noise sources present in this pixel sample before addition increase with $\sqrt{n_{\text{TDI}}}$. Noise sources that are present in the voltage signal are the following:

1) $1/f$ and random telegraph signal noise in the pixel source follower;
2) dark current shot noise;
3) kTC noise of the sense node, in case when correlated double sampling cannot be deployed.

The first noise source is reduced by optimizing the source follower (order of magnitude for short correlated double-sampling

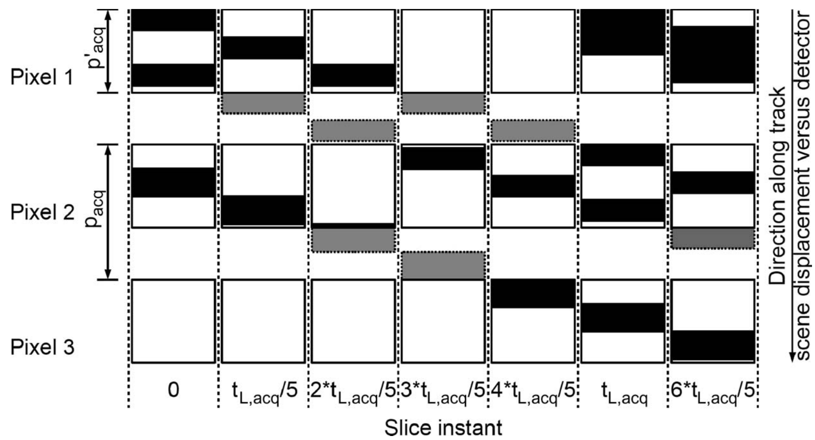

Fig. 12. Timing example: Scene displacement onto the device.

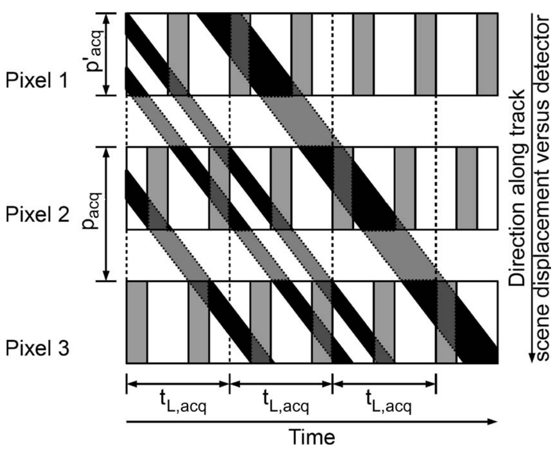

Fig. 13. Timing example: Synchronization of the samples.

operation: typically 4 electrons, it could be as low as 2 electrons) [7]. The last two noise sources are drastically reduced by the use of four-transistor pinned photodiode active pixels. Moreover, the temporal noise in the addition circuitry itself will increase by $\sqrt{n_{\mathrm{TDI}}}$ in the final output signal. Careful design of the analog chain and the adder circuit is required to lower as much as possible the overall read noise of the sensor.

The effect of voltage noise sources added in the pixel readout or addition circuits can be reduced by designing the pixel with a high conversion gain. This design approach is completely different from the design of TDI CCDs. In TDI CCD devices, each pixel must be designed to handle the full well charge of the final output signal. This imposes limitations as the design of pixels with a large charge capacity conflicts with the design of the best charge transfer efficiency. Finally, the full well charge of the TDI sensor is limited by the charge handling capacity in the horizontal CCD output channel and readout amplifier.

In CMOS image sensors, each pixel must be designed for the expected maximum charge that is acquired in one pixel only. Typically, this maximum charge level is rather low; this is the motivation to do TDI operation. The pixel is then designed with a large conversion gain in order to reduce the addition of extra noise sources after readout of the pixel. The total full well charge in the final output signal can be considerably larger, only

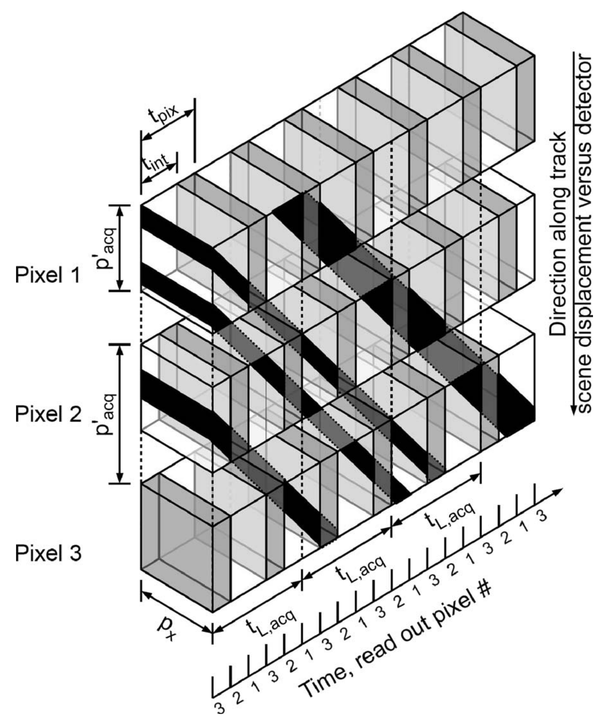

Fig. 14. Timing example: 3-D plot.

limited by the saturation levels in the addition circuitry. With digital addition circuits, there is virtually no limitation imposed by these circuits. Fig. 15 shows how the signal and noise relate to the number of TDI stages. The dynamic range and S/N ratio are increasing by 3 dB for every doubling in the number of TDI stages.

IV. Conclusion

Several conceptual architecture solutions for CMOS TDI sensors have been presented. If TDI is natural with CCD devices, it has potential shortcomings in CMOS: synchronization of the samples forming a TDI pixel, large matrix of adders outside the array, dynamic MTF or quantum efficiency reduction, not noise-free sample addition, and design complexity. However, there can be good reasons to use CMOS technology because of the advantage of process accessibility, reduced cost,

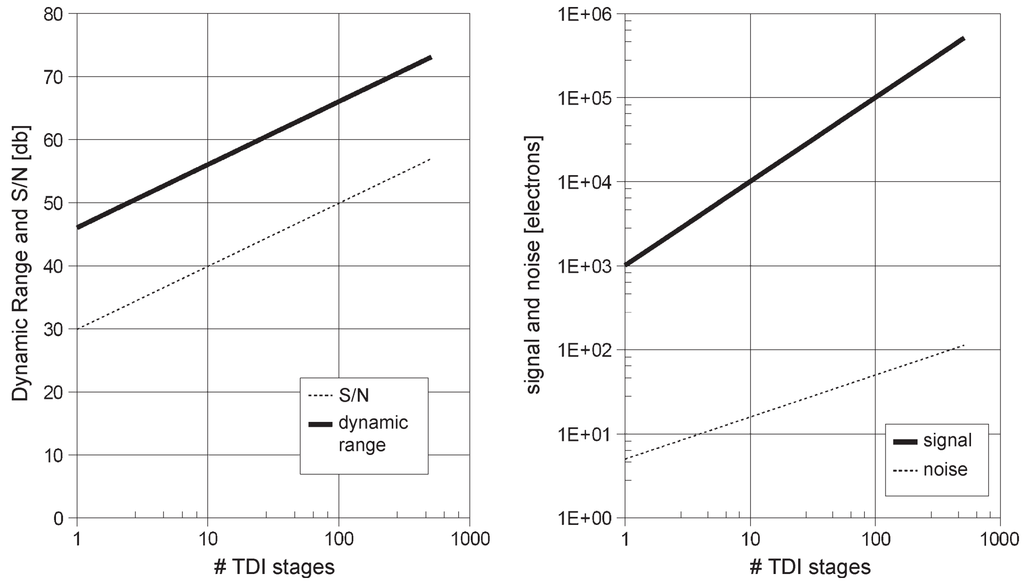

Fig. 15. Signal and noise in function of the number of TDI stage.

additional circuit functionality on-chip, robustness to ionizing radiation, simpler system design, etc. Existing and new TDI sensor architecture concepts with snapshot shutter, rolling shutter, or orthogonal readout have been presented. An optimization method has been introduced to inject MTF and quantum efficiency specification in the architecture definition. Moderate spatial and temporal oversamplings are combined to achieve near CCD class performances, resulting in an acceptable design complexity.

REFERENCES

[1] H.-S. Wong, Y. L. Yao, and E. S. Schlig, “TDI charge-coupled devices: Design and applications,” *IBM J. Res. Develop.*, vol. 36, no. 1, pp. 83–105, Jan. 1992.

[2] J. F. Johnson, “Modeling imager deterministic and statistical modulation transfer functions,” *Appl. Opt.*, vol. 32, no. 32, pp. 6503–6513, Nov. 1993.

[3] B. Pain, T. Cunningham, G. Yang, M. Ortiz, and B. Olson, “CMOS image sensors capable of time-delayed integration,” *NASA Tech Briefs*, vol. 25, no. 4, Apr. 2001, NPO-20802.

[4] G. Lepage, D. Dantès, and W. Diels, “CMOS long linear array for space application,” in *Proc. Electron. Imag. Conf.*, Jan. 2006, vol. 6068, pp. 61–68.

[5] H. Bugnet, “Design and evaluation of TDI operation of CMOS sensor for industrial imaging application,” in *Proc. Minalogic Image Sens. Image Process.*, 2008.

[6] G. Lepage, “Time delayed integration CMOS image sensor with zero desynchronization,” Patent Application US 20080079830, Apr. 3, 2008.

[7] X. Wang, P. Rao, and A. Theuwissen, “Characterization of the buried channel n-MOST source followers in CMOS image sensors,” in *Proc. Int. Image Sens. Workshop*, Ogunquit, ME, Jun. 6–10, 2007.

[8] L. Wengao, G. Jun, C. Zhongiian, L. Jing, C. Wentao, T. Ju, and J. Lijiu, “A novel low-power readout structure for TDI ROIC,” in *Proc. 5th Int. Conf. ASIC*, 2003, vol. 1, pp. 591–594.

[9] C. B. Kim, B. H. Kim, Y. S. Lee, H. Jung, and H. C. Lee, “Smart CMOS charge transfer readout circuit for time delay and integration arrays,” in *Proc. IEEE Custom Integr. Circuits Conf.*, 2006, pp. 651–654.

[10] F. K. Tsai, H. Y. Huang, L. K. Dai, C. D. Chiang, P. K. Weng, and Y. C. Chin, “A time-delay-integration CMOS readout circuit for IR scanning,” in *Proc. 9th Int. Conf. Electron., Circuits Syst.*, 2002, vol. 1, pp. 347–350.

[11] H. Michaelis, R. Jaumann, S. Mottala, J. Oberst, R. Kramm, R. Roll, H. Boehnhardt, H. Michalik, and G. Neukum, “CMOS-APS sensor with TDI for high resolution planetary remote sensing,” in *Proc. IEEE CCD AIS Workshop*, 2005, pp. 31–34.

Gérald Lepage received the M.Sc. degree from Polytech’ Montpellier, Montpellier, France, in 2002.

In 2002, he joined FillFactory (later acquired by Cypress Semiconductor), where he worked on various custom image sensor designs, in particular on the first large TDI CMOS sensor and on a very efficient snapshot electronic shutter sensor. He also developed embedded analog-to-digital converters for image sensors. In the last years, he worked on various custom sensors for space applications. He quit Cypress Semiconductor in mid-2007. He is currently with CMOSIS, Antwerpen, Belgium, where he is a Cofounder. He is the holder of several patents and has coauthored several publications in the field of CMOS APS.

Jan Bogaerts received the M.Sc. and Ph.D. degrees in electrical engineering from the Catholic University of Leuven, Leuven, Belgium, in 1997 and 2002, respectively. His Ph.D. research focused on radiation-induced degradation effects in CMOS active pixel sensors and the design of radiation-tolerant image sensors.

In 1997, he started working as a Ph.D. student with IMEC, Leuven, in the group specialized in the design of CMOS imagers, receiving a grant from the Flemish Institute for the Support of Scientific and Technological Research in Industry (IWT). In 2001, he joined FillFactory (later acquired by Cypress Semiconductor), where he designed the first radiation-tolerant APS in the world and was involved in the development of more than 20 APS design projects for space, scientific, medical, and industrial applications. When he left Cypress Semiconductor at the end of 2006 to join IMEC, he was the Technical Lead of the custom design team in Mechelen. In his role as a Senior Designer at IMEC, he was involved in the development of 3-D integrated and backside illuminated CMOS APS. He quit IMEC in late 2007. He is currently with CMOSIS, Antwerpen, Belgium, where he is a Cofounder. He is the holder of several patents and has coauthored about 20 publications in the field of CMOS APS.

Guy Meynants received the M.Sc. and Ph.D. degrees in electronics engineering from the Catholic University of Leuven, Leuven, Belgium, in 1994 and 1998, respectively.

Between 1994 and 1999, he was with IMEC, Leuven, working on CMOS active pixel image sensors. He was one of the Cofounders of FillFactory NV in 2000, where he developed various CMOS image sensors for industrial, digital photography, and space applications. He designed the 14-megapixel image sensors used in the Kodak Professional 14n, SLR/n, and SLR/c digital cameras, at that time (2002) the highest resolution digital SLR cameras on the market. In 2004, after Cypress Semiconductor acquired FillFactory, he focused on technology development for low-noise pixel architectures. From February 2006 to October 2007, he was with IMEC-NL, working on the research about ultralow-power analog circuits. Since 2007, he has been with CMOSIS, Antwerpen, Belgium, where he is a Cofounder, developing advanced professional image sensors. He is the holder of four patents and has several patent applications in the field of image sensors and analog circuit design. He has coauthored 40 publications. His current research areas are in the field of low-noise active pixels, large-area image sensors, and global shutter CMOS pixels.